

Conductance of a molecule with a center of mass motion

J. Mravlje,¹ A. Ramšak,^{1,2} and T. Rejec^{1,2,3}

¹*Jožef Stefan Institute, Ljubljana, Slovenia*

²*Faculty of Mathematics and Physics, University of Ljubljana, Slovenia*

³*Department of Physics, Ben-Gurion University, Beer-Sheva, Israel*

(Received 6 September 2006; revised manuscript received 3 October 2006; published 16 November 2006)

We calculate the zero temperature conductance and characteristic correlation functions of a molecule with a center of mass (c.m.) motion which modulates couplings to the leads. In the first model studied, the c.m. vibrational mode is simultaneously coupled to the electron density on the molecule. The conductance is suppressed in regimes corresponding to noninteger occupancy of the molecule. In the second model, where the c.m. mode is not directly coupled to the electron density, the suppression of conductance is related to the dynamic breaking of the inversion symmetry.

DOI: [10.1103/PhysRevB.74.205320](https://doi.org/10.1103/PhysRevB.74.205320)

PACS number(s): 73.23.-b, 72.15.Qm, 73.22.-f

I. INTRODUCTION

Interest in systems with electron-phonon interaction has recently reemerged, as a consequence of advances in experimental techniques enabling the investigation of the subtle interplay of electronic and vibrational degrees of freedom by means of measuring the conductance of the molecules.¹⁻¹³ Consequently, a considerable amount of work was done in pursuit of understanding the equilibrium¹⁴⁻¹⁷ and nonequilibrium¹⁸⁻²⁰ properties of these systems. The analysis of low-temperature properties of such systems is challenging as strong repulsive interaction among electrons confined to molecular orbitals leads to surprising results such as the interplay of the Kondo physics and molecular vibrations, which are intractable to conventional perturbational approaches. Investigation of the molecules which, when attached to the leads, may possess both internal and center-of-mass (c.m.) vibrational modes, makes the calculation of various properties even more involved.

Here we consider a molecule undergoing a linear transport measurement—a system which consists of a molecule and attached leads. The shape of the molecule and its position with respect to the leads oscillate (the setup is sketched in Fig. 1). Hence the orbital level of the molecule—for transport through molecules it is sufficient to consider a single orbital due to wide inter-level spacings⁷—and the tunneling amplitude are both modulated. Here we treat two possibilities: (i) in case I (proposed in Ref. 21) the vibrational mode that modulates the tunneling amplitude is also coupled to the electron density at the molecule; (ii) in case II (treated also in Ref. 22) the molecule possesses in addition to the c.m. mode a breathing mode which modulates the energy level of the molecular orbital.

Experimentally, c.m. modes are discerned in nonlinear transport measurements as sidebands in conductance which correspond to frequencies which do not match any of the eigenmodes of a given molecule. While the relevance of the separate couplings to two vibrational modes in model II is intuitively clear, the relevance of the simultaneous modulation of tunneling and coupling to the electron density in model I is less clear and deserves further exploration. We note that the model I could be relevant for the nonlinear

transport measurement where the electric field would directly couple to the electron density at the molecule, or in the presence of some impurities with residual electrical fields even in the (near) linear transport measurements.

The case of a molecule without the c.m. oscillations described by the Anderson-Holstein Hamiltonian has already been analyzed by several authors (see, e.g., Ref. 17 and references therein). The dominant effect of the coupling to the breathing mode is the reduction of the repulsive interaction among electron pairs occupying the molecular orbital. When the reduced repulsion U_{eff} is positive, a gate-voltage sweep reveals the area (of width of order U_{eff}) of enhanced linear conductance due to the Kondo effect. With increased electron-phonon coupling and thereby decreased U_{eff} this area is diminished. In this paper we show that the c.m. oscillations suppress the conductance in a new way which cannot be described by an effective model with reduced repulsion.

This paper is organized as follows. Section II introduces two related electron-phonon models. In Sec. III numerical methods based on the variational wave function are presented and some symmetry properties of the models are considered. In Sec. IV results for linear conductance for both models are presented and some ground state properties of the molecular system are explained. Results are summarized in Sec. V.

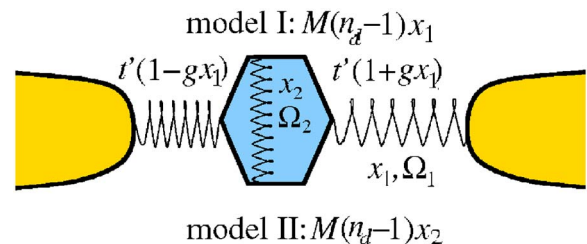


FIG. 1. (Color online) Schematic plot of the model devices. In model I the c.m. vibrational mode which modulates the tunneling amplitude t' is coupled also to the local charge density n_d . In model II the c.m. displacement modulates only the tunneling amplitude whereas another (breathing) vibrational mode is coupled to the local charge density.

II. MODELS

Hamiltonians for both models consist of the electron, the phonon and the electron-phonon coupling terms, $H=H_e+H_p+H_{e-p}$. In the electronic part of the Hamiltonian,

$$H_e = H_L + H_R + \epsilon_d n_d + U n_{d\uparrow} n_{d\downarrow} - t' (\hat{v}_L + \hat{v}_R), \quad (1)$$

$H_{L,R} = -t \sum_{i \in L,R} c_i^\dagger c_{i+1} + \text{H.c.}$ describe the noninteracting tight-binding left-hand and right-hand leads, respectively, and ϵ_d is the energy level of the molecular orbital occupied by $n = \langle n_d \rangle$ electrons where $n_d = \sum_{\sigma} n_{d\sigma}$ with $n_{d\sigma} = d_{\sigma}^\dagger d_{\sigma}$. The characteristic scale of the repulsive interaction is U and the tunneling part with characteristic tunneling rate t' consists of operators $\hat{v}_l = \sum_{\sigma} c_{l\sigma}^\dagger d_{\sigma} + \text{H.c.}$ for $l=L,R$ which couple the molecular orbital to the first site on the left-hand and right-hand leads, respectively. In H_e only the coupling between the molecular orbital and even combinations of the left-hand and the right-hand lead orbitals (i.e., the symmetric channel) is present.

Vibrational modes are described with $H_p^I = \Omega_1 a_1^\dagger a_1$ and $H_p^{II} = \Omega_1 a_1^\dagger a_1 + \Omega_2 a_2^\dagger a_2$ for models I and II, respectively, and $a_{1,2}^\dagger$ are the phonon creation operators. The corresponding electron-phonon interaction is given by

$$\begin{aligned} \text{I, } H_{e-p}^I &= t' g (\hat{v}_L - \hat{v}_R) x_1 + M(n_d - 1) x_1, \\ \text{II, } H_{e-p}^{II} &= t' g (\hat{v}_L - \hat{v}_R) x_1 + M(n_d - 1) x_2, \end{aligned} \quad (2)$$

where $x_{1,2} = a_{1,2}^\dagger + a_{1,2}$ are the displacement operators.

III. METHODS

The ground state properties are determined using the Gunnarsson and Schönhammer projection-operator method.^{17,23,24} Here the Hamiltonian is diagonalized in the basis

$$|\Psi_{\lambda\{m_\alpha\}}\rangle = P_\lambda \prod_{\alpha} a_{\alpha}^{\dagger m_\alpha} |\tilde{0}\rangle, \quad (3)$$

which consists of projectors P_λ , $P_0 = (1 - n_{d\uparrow})(1 - n_{d\downarrow})$, $P_1 = \sum_{\sigma} n_{d\sigma}(1 - n_{d\bar{\sigma}})$, and $P_2 = n_{d\uparrow} n_{d\downarrow}$ and additional operators involving the operators in leads (for example, $P_3 = P_0 \hat{v}_L P_1$), which are applied to the state $|\tilde{0}\rangle$ corresponding to the phonon vacuum and the ground state of the auxiliary noninteracting Hamiltonian with renormalized local energy $\tilde{\epsilon}_d$ and hopping parameters $\tilde{t}'_{L,R}$. In the model I $\alpha=1$ and $\alpha=1,2$ for the model II. Due to the c.m. displacement which induces the coupling to the asymmetric channel, the renormalized couplings to the left-hand and right-hand lead are not necessarily equal. The chemical potential was set to the middle of the band. A sufficient number of variational operators (up to ~ 40) and excited phonon states (up to ~ 40) were used in order to obtain converged results in the parameter regimes presented here.

Zero temperature conductance was calculated by two related methods, both based on the ground state wave function expressed in the basis Eq. (3). In the first method it was calculated from the sine formula (SF),^{25,26} $G = G_0 \sin^2[(E_+ - E_-)N/4t]$, where $G_0 = 2e^2/h$ and E_{\pm} are the

ground state energies of a large auxiliary ring consisted of N noninteracting sites and an embedded interacting system (molecule), with periodic and antiperiodic boundary conditions, respectively. In the second method we use the effective parameters of the auxiliary effective noninteracting Hamiltonian \tilde{H} and the conductance is then given from the corresponding Green's function (GF).²⁵ The advantage of the GF method is that the corresponding GF can be evaluated for infinite leads so the difficulties with convergence of SF with number of sites are avoided. However, the SF method is robust and it depends only on the accuracy of the ground-state energy which improves with the size of the basis in a transparent way. By comparing results of both methods we checked for the consistency and the convergence. From the effective parameters the conductance can also be calculated using the Friedel sum rule valid in the limit of large bandwidth ($t \gg U, M, \Omega_i, \dots$). When the coupling of the system between left-hand and right-hand lead differ, conveniently parametrized as $\tilde{t}'_L = (1+b)\tilde{t}'$, $\tilde{t}'_R = (1-b)\tilde{t}'$, the conductance is given by

$$\frac{G}{G_0} = \frac{(1-b^2)^2}{(1+b^2)^2} \sin^2 \frac{\pi}{2} n. \quad (4)$$

Note that conductance may be less than unity when both the symmetric and the antisymmetric channel participate in the transport (i.e., when $b \neq 0 \wedge b \neq \pm \infty$).

The asymmetry stems from the coupling to the c.m. displacement, hence the expectation values of the c.m. displacement $x = \langle x_1 \rangle$, and the calculated asymmetry factor b are related. More precisely, the following exact^{15,27} relations hold:

$$\text{I, } \langle x_1 \rangle = -\frac{2gt'}{\Omega_1} \langle \hat{v}_L - \hat{v}_R \rangle - \frac{2M}{\Omega_1} (n-1),$$

$$\text{II, } \langle x_1 \rangle = -\frac{2gt'}{\Omega_1} \langle \hat{v}_L - \hat{v}_R \rangle, \quad \langle x_2 \rangle = -\frac{2M}{\Omega_2} (n-1). \quad (5)$$

When $n=1$ the displacement x is proportional to the activity of the antisymmetric channel $\langle \hat{v}_L - \hat{v}_R \rangle$ for both models.

Some general conclusions may already be drawn from considering the particle-hole symmetry. Model I is invariant with respect to the particle-hole transformation $c_{i\sigma}^\dagger \rightarrow (-1)^i c_{i\bar{\sigma}}, d_{\sigma}^\dagger \rightarrow d_{\sigma}$ with $(\epsilon_d + U/2) \rightarrow -(\epsilon_d + U/2)$, and $x_1 \rightarrow -x_1$. Hence at the point of particle-hole symmetry (where $n=1$), $x=0$, therefore $b=0$ and conductance is unity according to the Friedel sum rule Eq. (4). The particle-hole transformation of model II yields $x_2 \rightarrow -x_2$ with no bounds on x_1 . The conductance of model II in the symmetric point therefore cannot be deduced from considering the particle-hole symmetry alone and may be less than unity there.

IV. NUMERICAL RESULTS

Throughout this paper we analyze the system with positive $U_{\text{eff}} = U - 2M^2/\Omega_\alpha$ and show the results for $U=10\Gamma$, $M=\Omega_\alpha=2.5\Gamma$, $U_{\text{eff}}=5\Gamma$, $\Gamma/t=2t'/t^2=0.08$, where $\alpha=1,2$ for model I and II, respectively. The scales of the values used correspond to typical molecular transistors.⁷

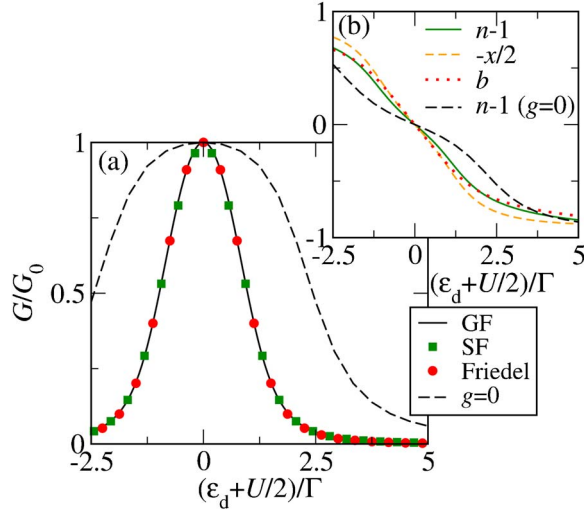


FIG. 2. (Color online) (a) Conductance as calculated from the Green's function corresponding to renormalized parameters (GF, full line), sine formula method with $N=3000$ (squares), and Friedel sum rule (circles) for molecules described by model I with $g=0.4$. For comparison, conductance for a molecule without coupling to the c.m. mode, $g=0$ (dashed line). (b) Local charge occupancy $n-1$ (full line), the displacement $x/2$ (short-dashed line), the asymmetry parameter b (dotted line) for a molecule described by model I with $g=0.4$, and the occupancy $n-1$ for $g=0$ (long-dashed line).

A. Model I

In Fig. 2(a) we show that all methods yield the same result for conductance within the model I (the same is true for model II discussed later). The area of enhanced conductance is diminished in comparison to the $g=0$ case. In general, the conductance curves calculated using different methods are very close. However, due to the finite bandwidth used here minor discrepancies in results applying the Friedel sum rule, Eq. (4), might occur when compared to other methods in the charge transfer and empty orbital regimes, $\epsilon_d + U/2 \gtrsim t$.

The results for the asymmetry factor b , the occupancy $n-1$ and the displacement x are shown in Fig. 2(b). As discussed above, the displacement at the symmetric point must vanish. Correspondingly, the asymmetry $b=0$ there. Near the particle-hole symmetric point we find the relation between the displacement and the asymmetry factor to be approximately linear.

We now systematically explain the properties of the ground state for model I starting from a Hamiltonian with $g=0$. In Fig. 3(a) we plot the conductance. Surprisingly, the influence of increasing g on the conductance is similar to simple reduction of U as is the case with the Anderson-Holstein model where the electron-phonon coupling term M effectively reduces U . However, as shown in Fig. 3(b) the occupancy n does not exhibit the sharp transition from $n \sim 2$ to $n \sim 0$ as seen in the Anderson model with reduced U_{eff} , where electron (or hole) pairs are preferred in the ground state (see, e.g., Ref. 17) and the transport is dominated by the pair tunneling.²⁸ In the strong coupling regime the occupancy preferentially takes on values near half-

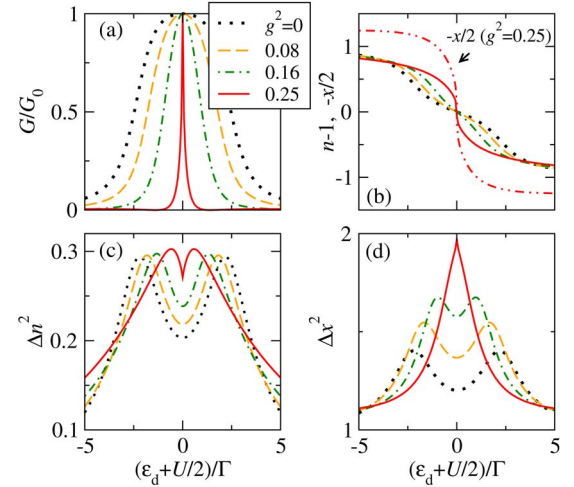


FIG. 3. (Color online) (a) Conductance of a molecule described by model I for various c.m. couplings g and fixed Holstein coupling M , $2M^2/\Omega_1=U/2$, $U=10\Gamma$, $M=\Omega_1=2.5\Gamma$. (b) The occupancy $n-1$ for various g . For $g^2=0.25$ also the average displacement $x/2$ (dashed-double-dotted line) plotted. (c) Fluctuations of charge $\Delta n^2 = \langle (n_d - n)^2 \rangle$ and (d) displacement $\Delta x^2 = \langle (x_1 - x)^2 \rangle$.

integer instead. This is because to the lowest order only the average displacement couples the electronic and phononic part, and the average displacement vanishes when $n=1$. Also, for states with well-defined occupancy $n \sim 0, 1, 2$, the hopping matrix element has a vanishing weight.

To illustrate this further we determined the charge fluctuations on the molecule. In general the range corresponding to increased charge fluctuations Δn^2 for $g > 0$ [Fig. 3(c)] is extended compared to the $g=0$ case. For large g the charge fluctuations still exhibit a minimum at the particle-hole symmetric point, in contrast to the negative- U (corresponding to strong coupling to the breathing mode) case where the charge analog of the Kondo effect with increased charge fluctuations evolves.¹⁷ The straightforward application of the fluctuation-dissipation theorem relates $\Delta n^2 \sim -\partial n / \partial \epsilon_d$, which does not apply to this system in some parameter regimes. On the other hand, the displacement fluctuations shown Fig. 3(d) are increased for large g at the symmetric point as in the Anderson-Holstein model.¹⁷

In Fig. 3(b) we also plot the average displacement $x/2$ of the molecule for $g=0.5$. According to the relation in Eq. (5), the difference between the occupancy (times $-2M/\Omega_1$) and the displacement x is determined by the difference between expectation values of the tunneling into left-hand and right-hand leads. At the symmetric point, this difference vanishes.

To summarize, in the particle-hole symmetric point the conductance is unity, contrary to the corresponding results presented in Ref. 21 where a dip in conductance was reported and related to the nonapplicability of the Friedel sum rule due to the breakdown of the Fermi liquid. Our results confirm that the conductance can be expressed with the Friedel sum rule, if left-right asymmetry is correctly taken into account, Eq. (4). The displacement of the oscillator in model I is determined by the occupancy. The displacement increases coupling to the antisymmetric channel and thereby the charge fluctuations which destroy the Kondo correlations

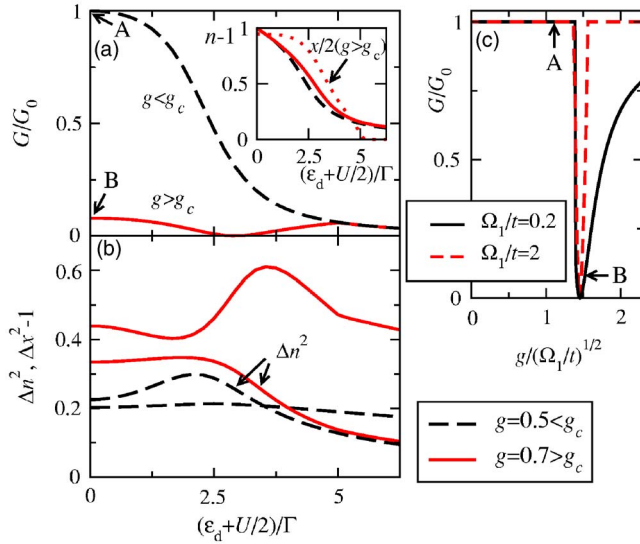


FIG. 4. (Color online) (a) Conductance of a molecule described by model II for $g < g_c$ (dashed) and $g_c < g < g'_c$ (full). $\Omega_1=0.2t$. Inset: The occupancy for the two cases. For $g > g_c$ also the c.m. displacement x is shown (dotted). For $g < g_c$ the c.m. displacement vanishes, $x=0$. (b) Fluctuations of charge and of c.m. displacement. The curve of charge fluctuations for $g=0.5$ is valid for all $g < g_c$. (c) The conductance in the symmetric point as a function of g .

with well-defined charge and enhanced conductance. Further, the displacement gives rise to asymmetry, which means conductance is additionally suppressed for general $\epsilon_d \neq -U/2$. The width of the conductance peak is seen to decrease approximately as $U - 2M^2/\Omega_1 - f(M, \Omega_1, t')g^2$ until this quantity is reduced to zero.

B. Model II

We now turn to the results within model II. For small enough values (to be quantified below) of the c.m. coupling $g < g_c$ the conductance is not significantly affected as unlike in model I the asymmetry is not determined (directly) by the occupancy of the molecule. The average displacement vanishes, correspondingly there is no asymmetry in the effective model; the width as well as the shape of the conductance peak and also the correlations exhibit only minor renormalization compared to the $g=0$ case. Conversely, for $g > g_c$ a soft mode emerges and the model has a transition reminiscent of dynamical Jahn-Teller distortion²² as within a simplified treatment of the related model.²⁹ This is signaled in our approach with nonvanishing x and asymmetry b in the effective model \tilde{H} and correspondingly with qualitatively modified correlations. For this regime additional variational basis functions might be required.³⁰ For c.m. coupling large enough, $g > g'_c$, only the asymmetric channel is active. This is a consequence of the renormalization: only the channel with the strongest Kondo coupling remains active at low temperatures, in accord with Ref. 22, and with corresponding unity conductance.

In Fig. 4(a) we plot the conductance and in Fig. 4(b) the fluctuations of occupancy and the displacement as a func-

tion of ϵ_d for two distinct $g_c < g < g'_c$ and $g < g_c$ and fixed $\Omega_1/t=0.2$. Whereas for $g < g_c$ the conductance and correlations are almost unaffected by the c.m. coupling (compare with the $g=0$ curves in Figs. 2 and 3), the $g > g_c$ result is markedly different. In the latter, the conductance is less than unity at the symmetric point and is zero at the point corresponding to $b=1$. In the inset of Fig. 4(b) we also plot the occupancy and for $g > g_c$ the c.m. displacement. For ϵ_d large enough, the c.m. displacement (and correspondingly the asymmetry) is zero. The precise value for g_c hence varies with the gate voltage and is related to the charge fluctuations of the bare model: increased charge fluctuations induce a transition to the state of spontaneously broken symmetry.

In Fig. 4(c) we plot the conductance as a function of coupling to the c.m. mode. For small g the conductance is unity as only the even channel is active, $b=0$. By increasing g , the conductance drops sharply at g_c which is found to be set by the relation $g_c^2 t/\Omega_1 = c(t')$, where $c(t') \sim 2.5$ for the results presented here.³¹ Note labels A and B indicating the values of g for which the results are shown in Figs. 4(a) and 4(b). For large Ω_1 both channels are active with corresponding suppressed conductance only for a narrow range of $g > g_c$ while for progressively decreasing Ω_1 the range of g with suppressed conductance widens. As in typical devices considered in experiments⁷ $\Omega_1 < \Gamma < U$ the anomalies in conductance of the type considered here would not be sensitive to the precise value of the coupling to the c.m. mode provided that it is large enough.

V. CONCLUSIONS

In conclusion, we analyzed the properties of molecules with a center of mass vibrational mode in linear transport measurements described by two distinct Hamiltonians. In the first case, where the coupling to the c.m. mode simultaneously modulates the molecular energy level, the result of the coupling to the c.m. mode is a reduced range of gate voltages with enhanced conductance. As a direct consequence of the particle-hole symmetry the conductance in the symmetric point remains unity.

In the second case where the coupling to the c.m. mode modulates only the tunneling matrix elements and additional breathing mode couples to the electron density, the c.m. mode is of minor relevance for the transport until a critical value of this coupling g_c is reached. For values of the coupling near the critical value anomalies due to the development of the soft mode arise signaled by the conductance which is less than unity. The conductance for these values is within our variational approach based on the effective model suppressed for a wide range of gate voltages.

We explained the relation of c.m. displacement to the transport of electrons for both models and substantiated the explanation by the numerical data for occupancy, occupancy fluctuations and also related phonon expectation values.

Finally, we may make some remarks regarding the experimental relevance of results presented here. For linear regime without residual electric fields it does not seem likely that the model I would provide an accurate description of the experimental situation. By analyzing model II which applies then,

we have shown that for small couplings to the c.m. mode there are no discernible effects on the linear conductance (we should note here that this statement would not be changed if additional breathing modes were introduced). At a sufficient coupling strength this picture changes: the displacement of the system from the point of inversion symmetry becomes increasingly sensitive to external perturbations which would result in a displacement of molecule and strong suppression of conductance.

To check for this behavior in experiments would require the following steps. First devices in which c.m. side peaks are seen would have to be produced, possibly by using different molecules, which would give in other respects identical devices besides having different frequencies of the c.m. motion. The fingerprint of the physics considered here would then be the suppression of conductance which would pre-

dominantly occur for the devices with lower frequencies of the c.m. motion. As this procedure would require near-atomic similar lead configuration near the molecule the systematic experimental confirmation of the analyzed effects seems currently hard to achieve. We speculate nevertheless that this effect might have contributed to the anomalously suppressed conductance in some of the devices considered in, e.g., Ref. 8.

ACKNOWLEDGMENTS

The authors thank R. Žitko for inspiring suggestions and S. El Shawish for discussions regarding the Jahn-Teller effect. The work was supported by SRA under Grant No. PI-0044.

-
- ¹V. Madhavan, W. Chen, T. Jamneala, M. F. Crommie, and N. S. Wingreen, *Science* **280**, 567 (1998).
- ²H. Park, J. Park, A. K. L. Lim, E. H. Anderson, A. P. Alivisatos, and P. L. McEuen, *Nature (London)* **407**, 57 (2000).
- ³J. Park *et al.*, *Nature (London)* **417**, 722 (2002).
- ⁴W. Liang, M. P. Shores, M. Bockrath, J. R. Long, and H. Park, *Nature (London)* **417**, 725 (2002).
- ⁵N. B. Zhitenev, H. Meng, and Z. Bao, *Phys. Rev. Lett.* **88**, 226801 (2002).
- ⁶L. H. Yu, Z. K. Keane, J. W. Ciszek, L. Cheng, M. P. Stewart, J. M. Tour, and D. Natelson, *Phys. Rev. Lett.* **93**, 266802 (2004).
- ⁷L. H. Yu and D. Natelson, *Nano Lett.* **4**, 79 (2005).
- ⁸A. N. Pasupathy *et al.*, *Nano Lett.* **5**, 203 (2005).
- ⁹A. Zhao *et al.*, *Science* **309**, 1542 (2005).
- ¹⁰J. Zhao, C. Zeng, X. Cheng, K. Wang, G. Wang, J. Yang, J. G. Hou, and Q. Zhu, *Phys. Rev. Lett.* **95**, 045502 (2005).
- ¹¹P. Wahl, L. Diekhoner, G. Wittich, L. Vitali, M. A. Schneider, and K. Kern, *Phys. Rev. Lett.* **95**, 166601 (2005).
- ¹²L. H. Yu, Z. K. Keane, J. W. Ciszek, L. Cheng, J. M. Tour, T. Baruah, M. R. Pederson, and D. Natelson, *Phys. Rev. Lett.* **95**, 256803 (2005).
- ¹³D. Natelson, L. H. Yu, J. W. Ciszek, Z. K. Keane, and J. M. Tour, *Chem. Phys.* **324**, 267 (2006).
- ¹⁴P. S. Cornaglia, H. Ness, and D. R. Grempel, *Phys. Rev. Lett.* **93**, 147201 (2004).
- ¹⁵P. S. Cornaglia, D. R. Grempel, and H. Ness, *Phys. Rev. B* **71**, 075320 (2005).
- ¹⁶P. S. Cornaglia and D. R. Grempel, *Phys. Rev. B* **71**, 245326 (2005).
- ¹⁷J. Mravlje, A. Ramšak, and T. Rejec, *Phys. Rev. B* **72**, 121403(R) (2005).
- ¹⁸A. Mitra, I. Aleiner, and A. J. Millis, *Phys. Rev. B* **69**, 245302 (2004).
- ¹⁹J. Paaske and K. Flensberg, *Phys. Rev. Lett.* **94**, 176801 (2005).
- ²⁰T. Yamamoto, K. Watanabe, and S. Watanabe, *Phys. Rev. Lett.* **95**, 065501 (2005).
- ²¹K. A. Al-Hassanieh, C. A. Büsser, G. B. Martins, and E. Dagotto, *Phys. Rev. Lett.* **95**, 256807 (2005).
- ²²C. A. Balseiro, P. S. Cornaglia, and D. R. Grempel, cond-mat/0605064 (to be published).
- ²³K. Schönhammer, *Phys. Rev. B* **13**, 4336 (1976).
- ²⁴K. Schönhammer and O. Gunnarsson, *Phys. Rev. B* **30**, 3141 (1984).
- ²⁵T. Rejec and A. Ramšak, *Phys. Rev. B* **68**, 035342 (2003).
- ²⁶T. Rejec and A. Ramšak, *Phys. Rev. B* **68**, 033306 (2003).
- ²⁷O. Gunnarsson and K. Schönhammer, *Phys. Rev. B* **31**, 4815 (1985).
- ²⁸J. Koch, M. E. Raikh, and F. von Oppen, *Phys. Rev. Lett.* **96**, 056803 (2006).
- ²⁹B. Alascio, C. Balseiro, G. Ortíz, M. Kiwi, and M. Lajos, *Phys. Rev. B* **38**, 4698 (1988).
- ³⁰A. C. Hewson and D. M. Newns, *J. Phys. C* **13**, 4477 (1980).
- ³¹In the symmetric point $g_c \sim 0.45\sqrt{\Omega_1/t/(t'/t)^{3/4}}$ irrespective of U , M , and Ω_2 .